Corrosion Behavior of 304L Stainless Steel Produced by Laser Powder Bed Fusion

Ho Lun Chan, Chemical Engineering

Mentor: Dr. Vilupanur Ravi

Kellogg Honors College Capstone Project

I. Background

Additive Manufacturing (AM)

- Process of joining materials to make objects from 3D model data, usually layer upon layer, as opposed to subtractive manufacturing methodologies. (ASTM F2792)
- The market revenue related to AM increased more than 14 times over the past two decades. Three popular industries for AM are **automotive, aerospace, and biomedical**.

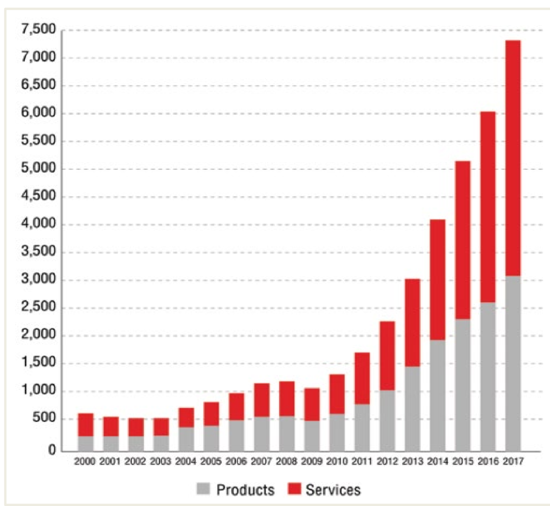

Figure 1. Revenue (USD $million) of products and services worldwide related to additive manufacturing

Laser Powder Bed Fusion (LPBF)

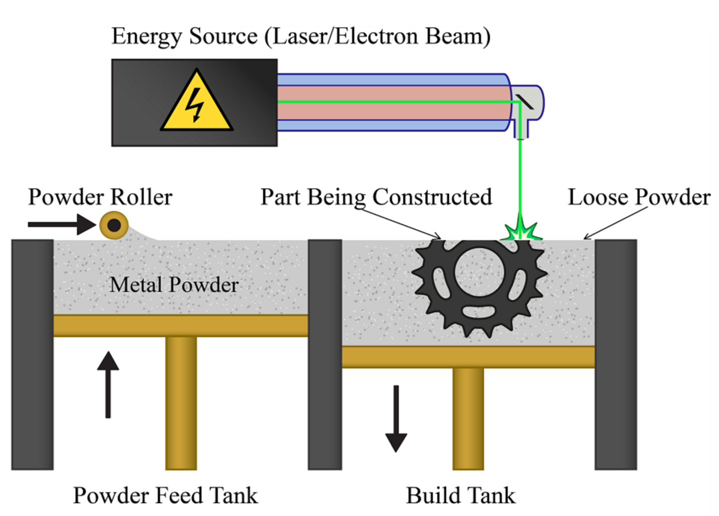

Figure 2. Schematics of Laser Powder Bed Fusion Process

Key Advantages:

- Control of part composition
- Direct parts production
- Fabricate geometrically intricate metallic parts
- Reduced waste compared to traditional casting

"The Corrosion Behavior of Metallic Alloys Fabricated by LPBF Is Not Well Characterized"

II. Objective

Study the corrosion behavior and microstructure of AM 304L Stainless Steel (SS) and its wrought counterpart under three conditions: as-fabricated, heat treated at 700°C for 250 hours, and heat treated at 800°C for 250 hours

III. Materials and Methods

Test Coupons (800 grit surface finish)

- Wrought 304L – As Received, 700°C/250h, 800°C/250 h
- AM 304L – As Built, 700°C/250h, 800°C/250h

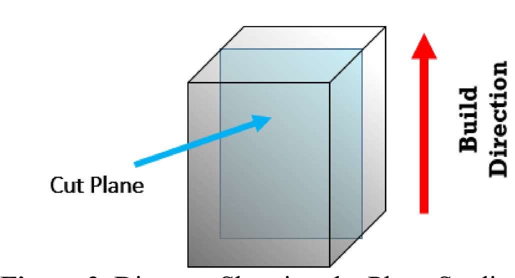

Figure 3. Diagram Showing the Plane Studied

Electrolyte

- Naturally Aerated 3.5 wt.% NaCl solution at 20°C

Corrosion Assessment

- **ASTM G59-97 + Tafel**: Determine corrosion rate
- **ASTM G61-86**: Determine resistance to pitting

Microstructural Characterization

- Scanning Electron Microscopy
- Energy Dispersive Microscopy

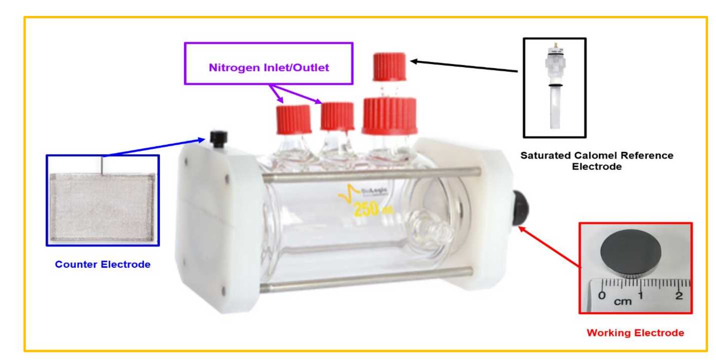

Figure 4. Corrosion Cell Setup

IV. Results and Discussion

Chemical Composition of Wrought and AM Alloy

Element (wt.%)	Fe	C	Cr	Cu	Mn	N	Ni	P	S	Si
Nominal	Balance	0.020	18.0-20.0	-	<2.00	-	8.0-12.0	<0.045	<0.030	<1.00
Wrought	Balance	0.022	18.3	0.510	1.43	0.079	8.120	0.033	0.024	0.350
AM	Balance	0.015	18.5	0.100	1.40	0.090	9.900	0.012	0.004	0.630

- Wrought alloy has higher amounts of carbon and sulfur
- AM alloy is composed of more silicon

Wrought vs. AM Alloys

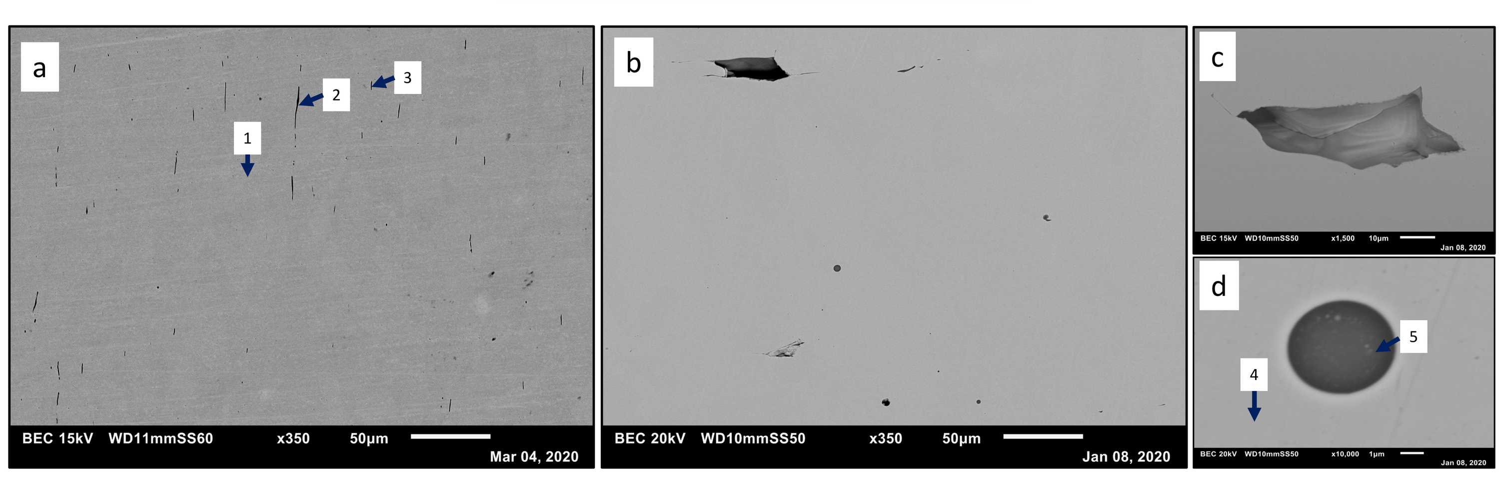

Figure 5. Backscattered electron micrographs of (a) as-received wrought and (b) as-built AM 304L alloys. Figures 5c and 5d show the typical microstructural defects observed in AM 304L alloys.

Table 1. Chemical Composition of Selected Points

Point	Atom fraction (at.%)								
	Fe	Cr	Ni	Mn	Ca	Si	Mg	O	S
1	69.6	20.4	7.47	1.6	-	-	-	-	-
2	10.3	5.5	1.12	41.2	-	-	-	-	41.9
3	7.4	3.0	0.9	2.5	8.1	11.5	5.7	49.1	0.14
4	68.5	19.7	9.03	1.69	-	1.15	-	-	-
5	1.14	6.87	-	13.6	0.27	13.5	-	64	-

- Manganese sulfides and oxide inclusions could be found in the stringer on the as-received wrought 304LSS alloy
- Fine oxide inclusions and pores due to lack of fusion were observed on as-built AM 304LSS alloy

Heat Treatment Effect on Microstructure and Corrosion

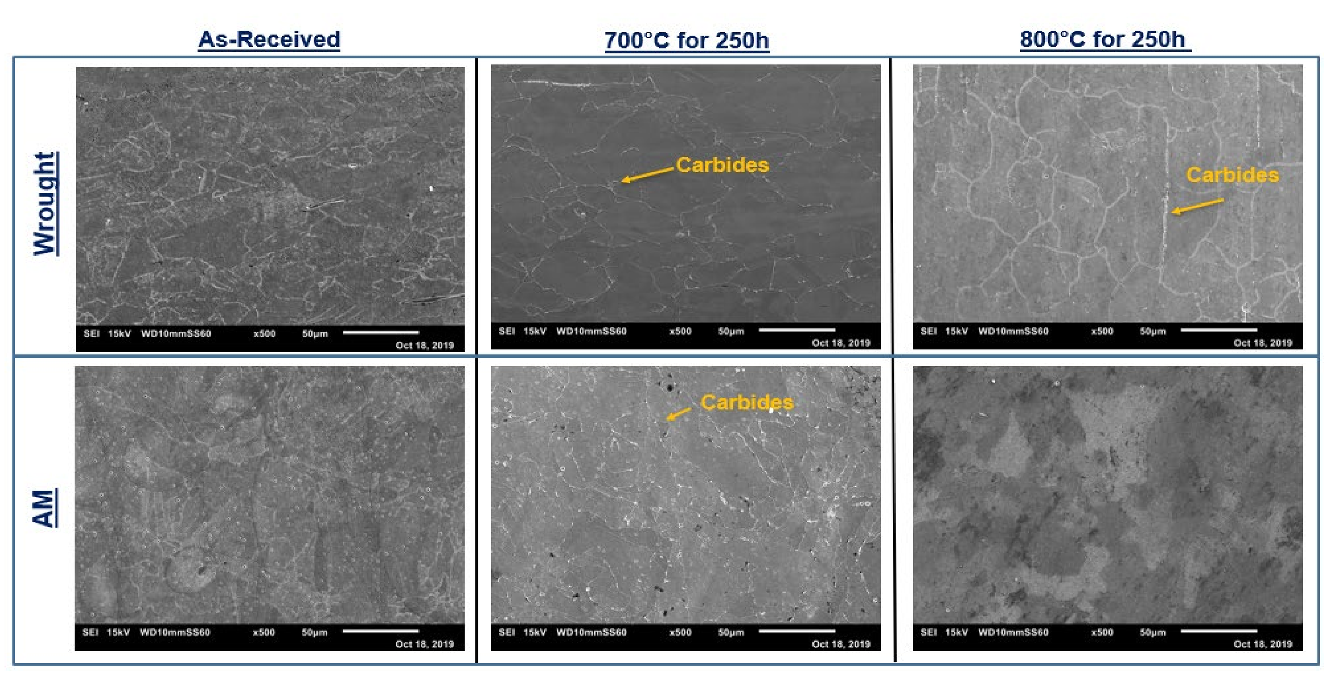

Figure 6. Backscattered electron micrographs of wrought and AM 304L alloys with and without heat treatment

- Carbide formation was observed on wrought and AM 304L alloys when heat treated at 700°C for 250 hours
- When heat treated at 800°C for the same duration, the formation of carbide is not apparent on the AM alloys.
- It is hypothesized that AM alloy is less sensitized compared to the wrought alloy due to the lower carbon contents seen in Table 1.

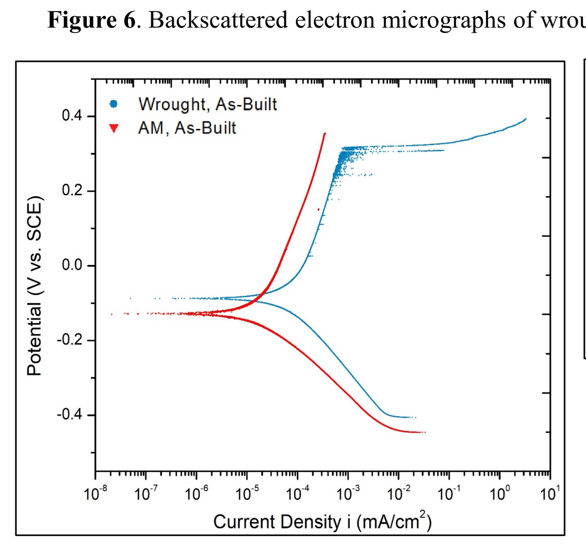

Figure 6. Representative Tafel Polarization Plot of wrought and AM 304L

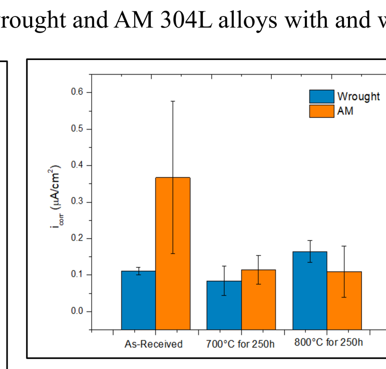

Figure 7. Calculated i_{corr} values

- Metastable pitting is observed on the AM 304 alloys
- Heat treatment reduces the corrosion rate (i_{corr}) for the AM 304L alloys

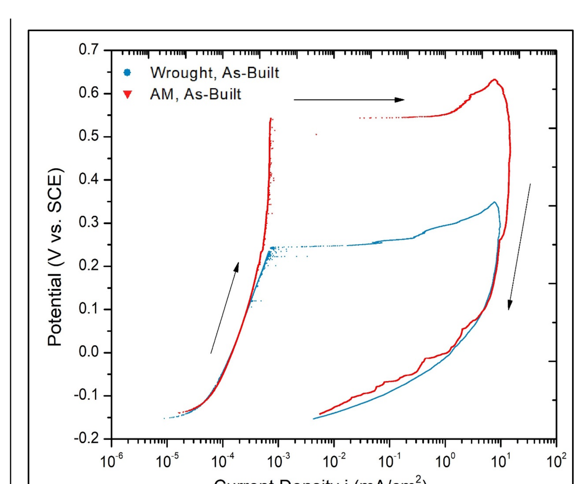

Figure 8. Representative Cyclic Potetiodynamic Polarization Plot of wrought and AM 304L

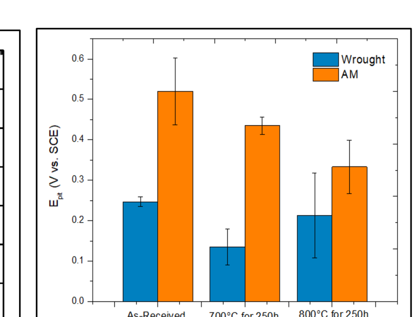

Figure 9. Pitting Potential (E_{pit})

- AM alloys show superior pitting resistance (E_{pit})
- E_{pit} is reduced when heat treated at 700°C for 250 hours. This is consistent with the carbide formation

V. Conclusion

- The corrosion behavior of wrought and additively manufactured 304LSS in 3.5 wt% NaCl was studied using electrochemical methods.
- The corrosion current of additively manufactured 304L SS are higher than that of its wrought counterpart. However, heat treatment reduces the corrosion current of AM alloys.
- Additively manufactured 304L SS shows higher resistance to pitting in chloride-containing environments possibly due to the lack of inclusion sites (MnS phase).
- Carbide formation was observed at 700 °C for 250 hours but not at 800 °C for the same time. The formation of carbides is likely to undermine the corrosion resistance of both wrought and AM alloys.
- Further investigation needs to be performed for AM 304L alloys heat treated at 800 °C for 250 hours.

VI. References

1. ASTM Standard F2792-10 (2010), West Conshohocken, PA: ASTM.
2. Wohlers Report 2018: 3D Printing and Additive Manufacturing State of the Industry, Wohlers Associates
3. D. Herzog, et al., *Acta Materialia* 117, (2016): p.371.
4. A. J. Sedriks, Hoboken, New Jersey: Wiley-Interscience Publication, 1996.
5. R. Unnikrishnan, et al., *Materials Characterization* 93, (2014): p.23.
6. A.S. Lima, et al., *Journal of Materials Science* 40, 1 (2015): p.139.
7. T. Amine, J. Newkrik (2019). 26th Annual International Solid Freeform Fabrication Symposium – An Additive Manufacturing Conference.
8. ASTM Standard G59-97 (2014), West Conshohocken, PA: ASTM.
9. ASTM Standard G61 - 86 (2018), West Conshohocken, PA: ASTM.
10. A. Jalbuena, et al. *JECS*, 166 (2019) 11
11. J. R. Trelewicz, et al., *JOM* 68, 3 (2016): p.850.
12. N. Ida, et al., *JECS*, 164, 13 (2017): p.C779.
13. R.F. Schaller, et al., *JECS*, 165, 5 (2018): p.C234.
14. R.M. Stoudt, et al., *JOM* 69, 3 (2017): p.506.

VII. Acknowledgements

I would like to thank my advisor Dr. Vilupanur Ravi for his continuous support, patience, and mentorship. I would also like to extend my gratitude to Joeshph Newkrik (Missouri University of Science and Technology), Christopher Faraj, Jacob Benoun, Nick Ury, Kevin Guo, Thu Nguyen, Juan Landa, Joey Tulpinski and Ulus Ekerman (Cal Poly Pomona) for their help. The author gratefully acknowledge financial support from Ms. Sylvia Hall, Drs. George and Mei Lai, the LA section of NACE International, Western States Corrosion Seminar, Western Area of NACE International, Cal Poly Pomona Office of Undergraduate Research, the NACE Foundation, The Boeing Company, Chevron Corporation, California Steel Industries Inc., the Southern California Chapter of the Association for Iron & Steel Technology .The SEM images and EDS analysis were made possible through a NSF MRI grant DMR - 1429674.